



27 June 2002

**CHEMICAL
PHYSICS
LETTERS**

Chemical Physics Letters 359 (2002) 453–459

www.elsevier.com/locate/cplett

Three-dimensional quantum time-dependent study of the photodissociation dynamics of $\text{Na} \cdots \text{FH}/\text{D}$

Gil Katz^a, Yehuda Zeiri^b, Ronnie Kosloff^{a,*}

^a Department of Physical Chemistry and the Fritz-Haber Research Center, The Hebrew University, 91904 Jerusalem, Israel

^b Department of Chemistry, Nuclear Research Center – Negev, P.O. Box 9001, Beer-Sheva 84190, Israel

Received 9 January 2002; in final form 2 April 2002

Abstract

A time-dependent three-dimensional nonadiabatic computation study of the photodissociation of the van der Waals $\text{Na} \cdots \text{FH}$ molecule was performed for total $J = 0$. A very low probability of photo-reaction to produce $\text{NaF} + \text{H}$ was observed from most initial conditions. Enhancement of the $\text{NaF} + \text{H}$ product was observed for the isotopically substituted $\text{Na} \cdots \text{FD}$. The three-dimensional calculations are in qualitative agreement with the two-dimensional previous study. Calculated excited state lifetimes were in the range of ~ 100 ps. Excitation of the bend and the van-der Waals stretch significantly shortened these lifetimes without increasing the reaction yield. © 2002 Elsevier Science B.V. All rights reserved.

1. Introduction

Photochemical reactions are unique because of the ability of the light field to switch the chemical process on and off. This property allows a choice of a specific stereochemical configuration before initiating the reaction. For binary chemical encounters, the weakly bound van der Waals molecule of the reactant can create a launching point for stereospecific photochemical reactions [1]. This idea is behind the experimental study of the photodissociation of the $\text{Na} \cdots \text{FH}$ [2], $\text{Li} \cdots \text{FH}$ [3] and $\text{Li} \cdots \text{FCH}_3$ [4] van der Waals molecules.

Using light to initiate a chemical reaction has additional consequences. Absorption of light in the

UV/visible region leads to excited electronic surfaces. Chemical encounters on excited electronic surfaces may go through a maze of multiple electronic surfaces. This is in contrast to typical chemical reactions which are well described on the ground electronic surface. A theoretical framework of reactions on multiple electronic surfaces should supply insight into the reaction mechanism, and time scales and also be able to predict product yields and lifetimes. An understanding of these photochemical reactions goes beyond the Born–Oppenheimer approximation and is a challenge to theory. By building on the success of quasi-classical trajectory methods in describing ground state dynamics, semiclassical approximations, which amend the classical trajectory with the nonadiabatic electronic transitions, seemed to be a promising direction. Thus a comprehensive semiclassical

* Corresponding author. Fax: +972-2-6513742.

E-mail address: ronnie@grid.fh.huji.ac.il (R. Kosloff).

study was performed for the $\text{Na}\cdots\text{FH} \rightarrow \text{NaF} + \text{H}$ photochemical reaction, by comparing different surface hopping approximations [5]. However all schemes studied gave a very high yield of reaction products in conflict with experimental observations. This discrepancy became the motivation for a collinear nonadiabatic quantum study [6]. Both quantum and semiclassical studies employed the two lowest potential energy surfaces using the same potentials and the diabaticization scheme of the semiclassical investigation. A substantial disagreement between the semiclassical and quantum mechanical methods was observed for the $\text{Na}\cdots\text{FH(D)}$ photodissociation. The branching ratio between reactive and nonreactive channels was qualitatively different. The quantum approach suggested that practically no reaction occurs unless the FH vibrational mode is excited to $v = 3$, while the semiclassical calculations predicted a reaction yield of 99% even at $v = 0$. The lifetime of the photoexcited state was another example of discrepancy between the quantum and quasi-classical calculations. Moreover, in the quantum calculation, replacement of H by D led to a marked increase in the reaction probability; in the semiclassical methods, on the other hand, the reaction probability diminished [6].

It is well documented that nonadiabatic dynamics is very sensitive to the dimensionality of the problem [7,8]. In addition, based on electronic structure calculations, the ground state of the $\text{Na}\cdots\text{FH}$ molecule is bent [3]. Since the comparison between the fully quantum calculation and the semiclassical methods was restricted to a collinear configuration, it became necessary to extend the investigation to three dimensions.

The present work reports the results of three-dimensional (3D) quantum mechanical simulations of the $\text{Na}\cdots\text{FH(D)}$ photodissociation process. The purpose is to calculate reaction yields, excited state lifetimes and final state distributions.

2. Details of calculations

The dynamics of the photodissociation was simulated by solving the multi-surface time-dependent Schrödinger equation

$$i\hbar \frac{\partial}{\partial t} \begin{pmatrix} \tilde{\psi}_c \\ \tilde{\psi}_g \end{pmatrix} = \tilde{\mathbf{H}} \begin{pmatrix} \tilde{\psi}_c \\ \tilde{\psi}_g \end{pmatrix}. \quad (2.1)$$

The dynamics was generated by the Hamiltonian represented in a diabatic form

$$\tilde{\mathbf{H}} = \begin{pmatrix} \hat{\mathbf{T}} + \hat{\mathbf{V}}_c & \hat{\mathbf{V}}_{\text{int}} \\ \hat{\mathbf{V}}_{\text{int}} & \hat{\mathbf{T}} + \hat{\mathbf{V}}_g \end{pmatrix}. \quad (2.2)$$

The operation of the kinetic energy operator $\hat{\mathbf{T}}$ was executed using the Fourier method in Jacobi coordinates for total angular momentum $J = 0$

$$\hat{\mathbf{T}}_{\text{int}}(R, r, c) = -\frac{\hbar^2}{2\mu} \left(\frac{\partial^2}{\partial R^2} + \frac{\partial^2}{\partial r^2} + \left(\frac{1}{R^2} + \frac{1}{r^2} \right) \times \left((1 - c^2) \frac{\partial^2}{\partial c^2} + 2c \frac{\partial}{\partial c} \right) \right), \quad (2.3)$$

where R is the distance from the sodium atom to the center of mass of the HF, r is the HF distance and $c = \cos \theta$, where θ is the angle between the vectors associated with \vec{R} and \vec{r} . The volume element in these coordinates becomes: $d\mathcal{V} = dR dr dc$. The evaluation of the kinetic energy operator requires four fast Fourier transform (FFT) operations. The potential matrix elements $V_i(R, r, c)$, in the diabatic representation were taken from [5].

The Jacobi coordinate system of the reactant supplied an inappropriate description of the $\text{NaF} + \text{H}$ asymptotic photo-reaction product. For this reason, and to establish an internal check on convergence, the calculations were repeated employing other sets of coordinate systems such as perimetric, Eckart bond coordinates and Euclidean. The details of these implementations are described in [9].

3. Results and discussion

The photodissociation event was launched from a bound vibrational state on the ground electronic surface of the van der Waals complex. The low lying vibrational eigenstates were calculated using the relaxation method [11]. These calculations were performed on the ground electronic state of the nonadiabatic potential to supply an initial state. In addition the eigenstates of an improved

ground state potential were also calculated and compared to the results of [10]. These calculations verified the convergence and helped in the assignment scheme used to classify the vibrational eigenvalues according to low frequency Na...FH stretch, bend, and to high frequency FH stretch.

A simulation of the photodissociation dynamics, assuming a weak excitation field, can be carried out by promoting the wavefunction from the ground PES vertically to the excited electronic surface [12,13]. The subsequent dynamics of this wavepacket can be filtered to obtain the energy-dependent photodissociation cross-section. An alternative view is that the initial state is created by a short excitation pulse of duration τ , where $1/\tau \gg \Delta\omega$, where $\Delta\omega$ is the width of the absorption band. Employing this approach, the variation of the norm of the excited wavefunction as a function of time shown in Fig. 1, can serve as an indication of the lifetime of the excited complex. The overlap of the excited wavefunction with the initial wavefunction can be used to obtain the absorption spectrum [18]. The decay times are estimated by fitting the excited state norm to a decaying exponential.

As can be observed in Fig. 1, the decay at short times is faster. This means that the initial wavepacket contains resonances with a lifetime less than ~ 300 fs. The small oscillations are the result

of the nonadiabatic mixing. The lifetimes of the dominant contribution estimated at 1 ps have limited accuracy.

Compared to the 2D results, the decay of the excited states in the 3D case is slightly faster. For example, for the Na...FH ground initial state $\psi(0,0,0)$ a lifetime of 121 ps is obtained in the 3D calculation compared to 172 ps in the 2D case. The notation used to define the initial state $\psi_i(i,j,k)$ corresponds to the three vibrational quantum numbers: i =HF/FD stretch, j =bending mode and k =Na...FH van der Waals stretch. For the Na...FD $\psi(0,0,0)$ initial state, the estimated decay time in the 3D case is 5.1 ps, compared to 6.6 ps in the 2D result.

A more precise estimation of the excited state lifetimes is obtained by decomposing the vertical Franck–Condon initial wavefunction to the contributions of the direct dissociation and resonances. The autocorrelation function $C(t) = \langle \psi(0) | \psi(t) \rangle$ includes all the dynamical information which evolves out of the initial wavefunction. By filtering $C(t)$ the contribution of the major resonances to the dynamics can be unraveled. The filter diagonalization (FD) approach [14–16] allows this dynamical information to be obtained from a finite time history. The outcome shown in Table 1 is a series of amplitudes, energies and lifetimes filtered out from the autocorrelation function, initiated by a specific initial wavefunction. The assignment of the resonances was done by noticing that the high frequency mode is still the FH stretch and that the bend and stretch low frequency modes can be compared to the assignments of the ground state wavefunctions [9,10]. The FH stretch frequency decreased from ~ 4500 cm^{-1} on the ground electronic surface, to ~ 3780 cm^{-1} upon excitation.

To create a basis for assigning the resonances, the first few eigenstates of the adiabatic excited state potential were calculated using the relaxation method [11]. These excited state eigenstates supplied nodal patterns and approximate frequencies of the two lowest energy modes, the bend and the Na–FH-stretch. These frequencies were compared to frequencies obtained by FD out of the autocorrelation function of a ground surface initial wavefunction promoted to the excited surface. The initial wavefunction was a direct product

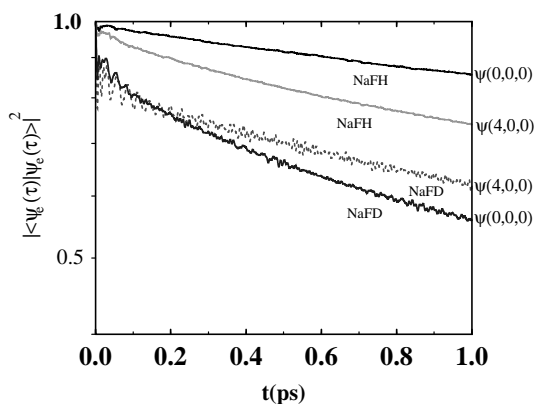


Fig. 1. A semi-log plot of the square of the wavefunction norm $\langle P_e \rangle = |\langle \psi_e(t) | \psi_e(t) \rangle|^2$ as a function of time for a ground state wavefunction of NaFH/D system promoted to the excited state. The initial wavefunction is indicated on the right-hand side.

Table 1

Lifetime, energies and relative amplitude obtained by the filter diagonalization method (FD) from the 3D autocorrelation function

Initial state	Possible assignment	Energy (cm ⁻¹) 3D-FD	Lifetime (ps) 3D-FD	Amplitude 3D-FD	Lifetime (ps) 3D-norm	Lifetime (ps) 3D-norm
$\psi_{\text{NAHF}}(0, 0, 0)$	$\psi_{\text{NAHF}}(0, 0, 0)$	0 (1976)	107.4	0.86	121	172
	$\psi_{\text{NAHF}}(0, 0, 1)$	112	21.30	0.05		
	$\psi_{\text{NAHF}}(0, 0, 2)$	204	12.3	0.02		
	$\psi_{\text{NAHF}}(0, 1, 0)$	171	7.54	0.02		
	$\psi_{\text{NAHF}}(0, 1, 1)$	287	6.54	0.03		
	$\psi_{\text{NAHF}}(0, 1, 2)$	374	1.76	0.006		
	$\psi_{\text{NAHF}}(1, 0, 0)$	3798	7.5	0.002		
	$\psi_{\text{NAHF}}(2, 0, 0)$	7245	5.3	0.0003		
	$\psi_{\text{NAHF}}(3, 0, 0)$	10 542	4.1	0.000007		
	$\psi_{\text{NAHF}}(4, 0, 0)$	13 622	1.7	0.000004		
$\psi_{\text{NAHF}}(4, 0, 0)$	$\psi_{\text{NAHF}}(0, 0, 0)$	(1979)	109	0.05		
	$\psi_{\text{NAHF}}(0, 0, 1)$	109	23.90	0.09		
	$\psi_{\text{NAHF}}(0, 0, 2)$	198	11.7	0.08		
	$\psi_{\text{NAHF}}(0, 1, 0)$	168	7.1	0.02		
	$\psi_{\text{NAHF}}(0, 1, 1)$	284	6.7	0.04		
	$\psi_{\text{NAHF}}(0, 1, 2)$	371	1.81	0.009		
	$\psi_{\text{NAHF}}(1, 0, 0)$	3721	7.65	0.27		
	$\psi_{\text{NAHF}}(2, 0, 0)$	7257	5.9	0.09		
	$\psi_{\text{NAHF}}(3, 0, 0)$	10 598	4.3	0.06		
	$\psi_{\text{NAHF}}(4, 0, 0)$	13 634	1.7	0.36	30	27
$\psi_{\text{NaDF}}(0, 0, 0)$	$\psi_{\text{NaDF}}(0, 0, 0)$	0 (1171)	3.3	0.39	5.1	6.6
	$\psi_{\text{NaDF}}(1, 0, 0)$	3169	1.84	0.22	–	–
	$\psi_{\text{NaDF}}(2, 0, 0)$	6081	1.27		0.13	–
	$\psi_{\text{NaDF}}(3, 0, 0)$	8945	0.66	0.08		–
	$\psi_{\text{NaDF}}(4, 0, 0)$	10 760	0.53	0.2	2.7	–

The lifetimes are compared to the those obtained by fitting the norm to an exponential decay. The energies are relative to the first peak whose value is indicated in bold. The assignment used is: ψ (HF-stretch, bend, Na–FH-stretch).

wavefunction composed from the HF stretch wavefunctions and the ground state bend and Na–FH-stretch on the ground electronic surface. To assist the assignment an initial state was used starting from the ground vibrational state on the upper adiabatic potential. To this state an additional momentum kick in the direction of the bend or to the Na–FH-stretch was applied. By com-

paring the changes in amplitudes of the frequencies obtained in the FD method for different initial states the frequencies were assigned to normal modes. Due to intermode coupling for excited states this assignment is only approximate. Once frequencies were identified, the FD procedure was repeated with a smaller frequency window which led to higher resolution.

Table 2

Branching ratio between product and reactant channels

The channels	Initial state	3D	2D
(NaF + H)/(Na + FH)	$\psi(0, 0, 0)$	0.00036	0.0002
(NaF + H)/(Na + FH)	$\psi(0, 1, 0)$	0.000394	
(NaF + H)/(Na + FH)	$\psi(4, 0, 0)$	0.2058	110 000
(NaF + D)/(Na + FD)	$\psi(0, 0, 0)$	0.38461	0.315
(NaF + D)/(Na + FD)	$\psi(4, 0, 0)$	0.741077	–

The longest lifetimes of the resonances obtained by the FD method are in good agreement with the lifetime obtained from the decay of the norm. The results presented in Table 1 clearly show that excitations of the bend and the $\text{Na} \cdots / \text{FH}$ stretch modes shorten the excited state lifetimes. Nevertheless these excitations do not lead to an increase in the reaction yield, which means that the decay of the norm is due to leaks through nonadiabatic transitions back to the reactant channels (cf. Table 2) on the ground electronic state.

The branching ratios between the products $\text{NaF} + \text{H}$ and the reactants $\text{Na} + \text{FH}$ was estimated from the ratio of the accumulated flux calculated at a dividing surface positioned in the asymptotic valleys. As can be seen in Fig. 2 the ratio stabilized after approximately 1 ps. The bursts at 400 fs are

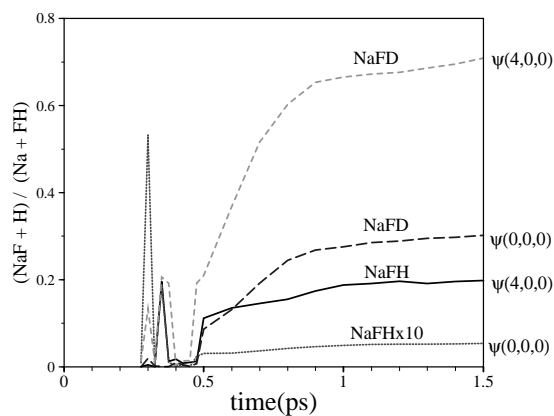


Fig. 2. The accumulated flux ratio between reactants and products as a function of time for different initial wavefunctions.

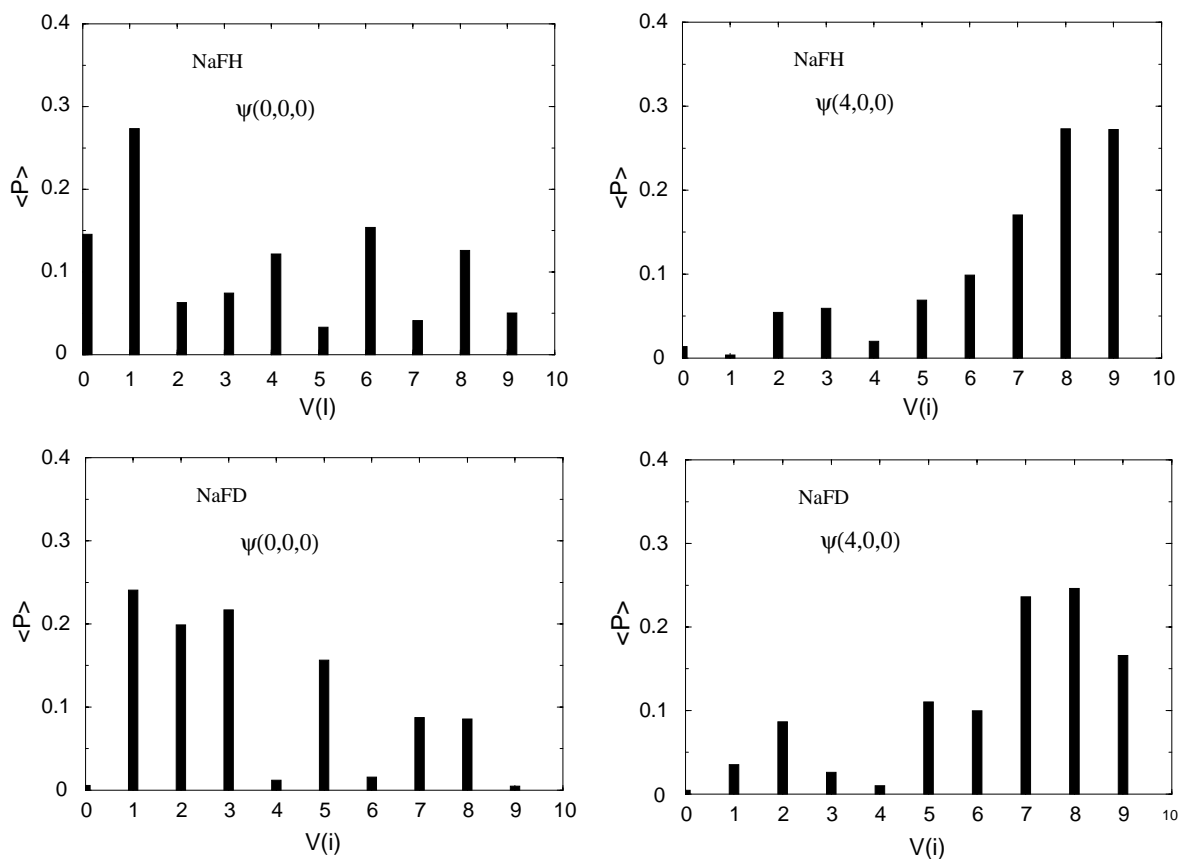


Fig. 3. The final vibrational distribution of the NaF products starting from $\text{Na} \cdots \text{FH}$ and $\text{Na} \cdots \text{FD}$.

the result of flux from fast direct reaction. The overall contribution of this component in the accumulated flux is very small.

From a qualitative point of view, the 3D results are similar to the 2D ones. The reaction probability is also found to be strongly influenced by isotopic substitution. The branching ratio between the reactant and product channels is shown in Table 2 where the 3D data are compared to the 2D results.

The qualitative trends in the 3D calculations are similar to the 2D results. However the enhancement of the reaction product formation upon HF stretch excitation and the isotope substitution is less pronounced.

Starting with specific initial states a final state analysis was performed at the asymptotes. The analysis extracted the translational energy distribution of the products by a Fourier transform of the wavefunction in the asymptotic channel. The final vibrational distribution of the NaF was evaluated by accumulating the flux of the projected wavefunction on the asymptotic vibrational states.

The final state vibrational distribution of NaF is shown in Fig. 3.

These results indicate that exciting the initial HF/D vibration results in a much hotter product vibrational distribution for both isotopes. Fig. 4 shows the final translational energy distribution.

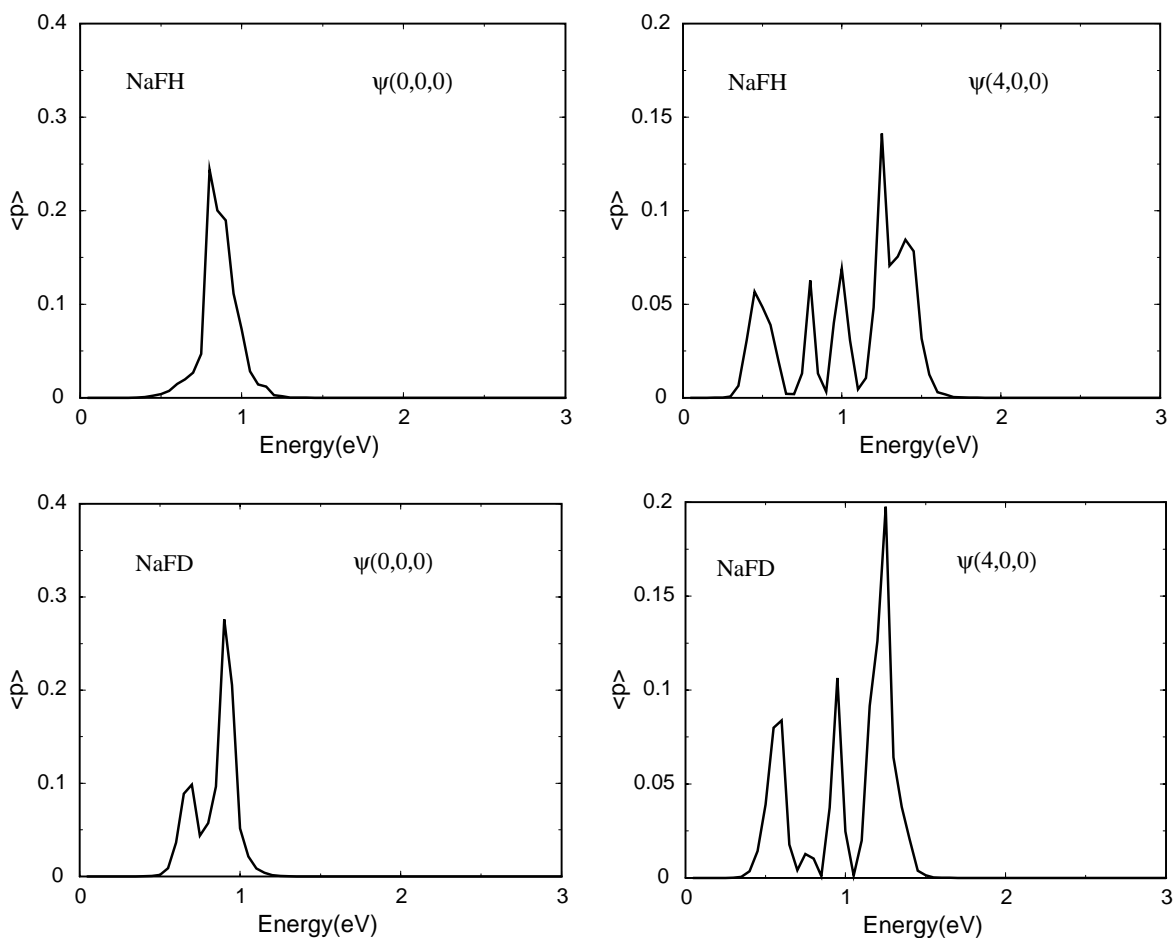


Fig. 4. The translational distribution of the Na...F-H/D relative motion.

The final translational distribution seems to reflect a mapping of the FH initial vibration wavefunction. This observation can be rationalized by the light hydrogen atom which is responsible for most of the vibrational motion in the HF/D stretch. This is clearly manifested in the observed asymptotic relative translation.

4. Conclusions

To conclude, the 3D quantum calculations show the same general trends as the 2D calculations. This means that the bending motion due to its low frequency is a spectator to the other degrees of freedom. These findings still leave the large discrepancy in the product yield between the fully quantum and semiclassical calculations. In particular, the new semiclassical calculations [17] on an improved potential energy surface still show a very high yield of NaF products and very short excited state lifetimes. The central role played by the nonadiabatic effects in the dynamics suggests that a complete picture of the dynamics should include also the two nonreactive electronic excited states which correlate with the perpendicular *P* excitations on the sodium atom.

Acknowledgements

We thank J. C. Polanyi, D. Neuhauser and D. G. Truhlar for their help and assistance. This research was supported by the Israel Canada fund.

The Fritz Haber Research Center is supported by the Minerva Gesellschaft für die Forschung, GmbH München, Germany.

References

- [1] J. Zang, M. Dulligan, J. Segall, Y. Wen, C. Wittig, *J. Chem. Phys.* 99 (1995) 13680.
- [2] X.-Y. Chang, R. Erlich, A.J. Hudson, P. Piecuch, J.C. Polanyi, *Faraday Discuss. Chem. Soc.* 108 (1997) 411.
- [3] A.J. Hudson, H.B. Oh, J.C. Polanyi, P. Piecuch, *J. Chem. Phys.* 113 (2000) 9897.
- [4] A.J. Hudson, F.Y. Naumkin, H.B. Oh, J.C. Polanyi, S.A. Raspopov, *Faraday Discuss. Chem. Soc.* 118 (2001) 191.
- [5] M.S. Topaler, D.G. Truhlar, X.-Y. Chang, P. Piecuch, J.C. Polanyi, *J. Chem. Phys.* 108 (1998) 5349.
- [6] Y. Zeiri, G. Katz, R. Kosloff, M.S. Topaler, D.G. Truhlar, J.C. Polanyi, *Chem. Phys. Lett.* 300 (1999) 523.
- [7] D.R. Yarkony, *J. Phys. Chem. A* 105 (2001) 6277.
- [8] H. Nakamura, D.G. Truhlar, *J. Chem. Phys.* 115 (2001) 10353.
- [9] G. Katz, K. Yamashita, Y. Zeiri, R. Kosloff, *J. Chem. Phys.* 116 (2002) 4403.
- [10] V. Spirko, P. Piecuch, O. Bludsky, *J. Chem. Phys.* 112 (2000) 189.
- [11] R. Kosloff, H. Tal-Ezer, *Chem. Phys. Lett.* 127 (1986) 223.
- [12] R. Schinke, *Photodissociation Dynamics*, Cambridge University, Cambridge, 1993.
- [13] G.G. Balint-Kurti, R.N. Dixon, C.C. Marston, *J. Chem. Soc. Faraday Trans.* 86 (1990) 1741.
- [14] M.R. Wall, D. Neuhauser, *J. Chem. Phys.* 102 (1995) 8011.
- [15] J.W. Pang, T. Dieckmann, J. Feigon, D. Neuhauser, *J. Chem. Phys.* 108 (1998) 8360.
- [16] V.A. Mandelshtam, *J. Chem. Phys.* 108 (1998) 9999.
- [17] A.W. Jasper, M.D. Hack, A. Chakraborty, D.G. Truhlar, P. Piecuch, *J. Chem. Phys.* 115 (2001) 7945.
- [18] D.J. Tannor, E.J. Heller, *J. Chem. Phys.* 77 (1982) 202.